Adaptive Robust Precision Motion Control of a High-Speed Industrial Gantry With Cogging Force Compensations

Bin Yao, *Senior Member, IEEE*, Chuxiong Hu, *Student Member, IEEE*, Lu Lu, and Qingfeng Wang

***Abstract*—This paper studies the precision motion control of a high-speed/acceleration linear motor driven commercial gantry which is subject to significant nonlinear cogging forces. A discontinuous projection based desired compensation adaptive robust controller (DCARC) is constructed. In particular, based on the special structures of various nonlinear forces, design models consisting of known basis functions with unknown weights are used to approximate those unknown nonlinear forces with approximation errors being explicitly accounted for in the design process. Online parameter adaptation is then utilized to reduce the effect of various parametric uncertainties while certain robust control laws are used to handle effects of various modeling uncertainties. Theoretically, the resulting controller achieves a guaranteed transient performance and final tracking accuracy in the presence of both parametric uncertainties and uncertain nonlinearities. In addition, in the presence of parametric uncertainties, the controller achieves asymptotic output tracking. Comparative experimental results obtained on a high-speed Anorad commercial gantry with a linear encoder resolution of 0.5 μm and a position measurement resolution of 20 nm by external laser interferometer are presented to verify the excellent tracking performance of the proposed control strategy.**

***Index Terms*—Adaptive robust control (ARC), linear motor, motion control.**

I. Introduction

SIGNIFICANT efforts have been devoted to solving the difficulties in controlling linear motors [1], [3], [5]–[10], [13], [15], [22], [23], [30] due to the hardware advantages of such a system for use in high-speed/high-accuracy positioning systems. In [1], Alter and Tsao present a comprehensive design approach for the control of linear-motor-driven machine tool axes. H_∞ optimal feedback control is used to provide high dynamic stiffness to external disturbances (e.g., cutting forces in machining). Practically, H_∞ design may be conservative for high-speed/high-accuracy tracking control and there is no systematic way to translate practical information about plant uncertainty and modeling inaccuracy into quantitative terms that allow the application of H_∞ techniques. In [13], a disturbance compensation method based on disturbance observer (DOB) is proposed to make the linear motor system robust to model uncertainties. It is shown both theoretically and experimentally by Yao, *et al.* in [26] that DOB design may not handle discontinuous disturbances such as Coulomb friction well and cannot deal with large extent of parametric uncertainties. To reduce the nonlinear effect of force ripple, in [3], feedforward compensation terms, which are based on an offline experimentally identified model of first-order approximation of ripple forces, are added to the position controller. Since not all magnets in a linear motor and not all linear motors of the same type are identical, feedforward compensation based on offline identification model may be too sensitive and costly to be useful. In [18], a neural-network-based learning feedforward controller is proposed to reduce positional inaccuracy due to reproducible ripple forces or any other reproducible and slowly varying disturbances over different runs of the same desired trajectory (or repetitive tasks). However, overall closed-loop stability is not guaranteed. In fact, it is observed in [18] that instability may occur at high-speed movements. Furthermore, learning process may take too long to be useful due to the use of a small adaptation rate for stability. In [25], the idea of adaptive robust control (ARC) [24], [27], [28] is generalized to provide a rigorous theoretic framework for the precision motion control of linear motors. The controller takes into account the effect of model uncertainties coming from the inertia load, friction, force ripple and electrical parameters, etc. In [22] and [23], the proposed ARC algorithm [25] is applied on an *epoxy* core linear motor. To reduce the effect of velocity measurement noise, a desired compensation ARC algorithm in which the regressor is calculated by reference trajectory information is also presented and implemented.

In this paper, the proposed desired compensation ARC (DCARC) [22] will be extended to the control of a high-speed linear motor driven industrial gantry system with significant nonlinear cogging forces. For these types of linear motors, to have a smooth high-speed motion, it is necessary to explicitly compensate for the nonlinear cogging forces, which is the focus of this paper. As an alternative to feedforward force ripple compensation [3] or feedback compensation using measurements

Manuscript received July 31, 2008; accepted March 21, 2010. Manuscript received in final form August 18, 2010. Date of publication April 15, 2011; date of current version August 17, 2011. Recommended by Associate Editor R. E. Young. This paper was presented in part at the 2007 IEEE/ASME Conference on Advanced Intelligent Mechatronics, Zurich, Switzerland, September 4–7, 2007. This work was supported in part by the U.S. National Science Foundation under Grant CMMI-1052872, by the National Basic Research and Development Program of China under 973 Program Grant 2007CB714000, and by the Ministry of Education of China through a Chang Jiang Chair Professorship.

B. Yao is with the School of Mechanical Engineering, Purdue University, West Lafayette, IN 47907 USA, and also with State Key Laboratory of Fluid Power Transmission and Control, Zhejiang University, Hangzhou 310027, China (e-mail: byao@purdue.edu).

C. Hu is with The State Key Laboratory of Fluid Power Transmission and Control, Zhejiang University, Hangzhou 310027, China, and also with the Institute of Manufacturing Engineering, Department of Precision Instruments and Mechanology, Tsinghua University, Beijing 100084, China.

L. Lu and Q. Wang are with the The State Key Laboratory of Fluid Power Transmission and Control, Zhejiang University, Hangzhou 310027, China.

Color versions of one or more of the figures in this paper are available online at http://ieeexplore.ieee.org.

Digital Object Identifier 10.1109/TCST.2010.2070504

of back EMF [11], which may demand time-consuming and costly rigorous offline identification, one can reduce the effect of ripple forces by utilizing the particular physical structure of the ripple forces. Specifically, design models consisting of known basis functions with unknown weights are used to approximate the unknown ripple forces with online parameter adaptation to reduce the effect of various parametric uncertainties—similar idea has been used in [2] and [16] for the control of variable reluctance rotary motors. However, it should be noted that the underline control problem studied in [2] and [16] and the one here is totally different. Specifically, [2] and [16] assume the perfect modeling of the unknown ripple force by the known basis functions with unknown weights. As a result, the standard adaptive control algorithms can be applied to deal with the parametric uncertainties only. Theoretically, there always exists certain amounts of modeling errors, no matter how many numbers of basis functions are chosen. It is well known that the standard adaptation law may lose stability even when a small disturbance appears [19], and additional effort has to be made to safely implement those adaptive nonlinear controllers [2], [16]. One may apply remedies similar to those used in robust adaptive control [12]. However, such modifications do not guarantee tracking accuracy in the presence of disturbances, left alone transient performance. In contrast, this paper will explicitly consider the effect of modeling errors and use certain robust control laws to effectively deal with various modeling uncertainties. As a result, the proposed controller can theoretically achieve a guaranteed transient performance and a prescribed final tracking accuracy even in the presence of modeling errors, while preserving the asymptotic tracking capability of the ideal adaptive control law [29]. In addition, the proposed controller has several implementation advantages such as reducing the effect of measurement noise and having a faster adaptation process.

The proposed control strategy has been partially tested on an iron core linear motor in one of the first author's previous conference papers [21]. However, the linear encoder resolution of 1 μm and the maximum speed around 1 m/s of the iron core linear motor in [21] significantly limited its usefulness as an experimental testbed for high-speed/acceleration motions or slow motion with sub-micrometer positioning accuracy with cogging force compensation. To address this problem, a two-axes commercial high-speed gantry driven by linear motors with built-in linear encoder position measurement has recently been setup at Zhejiang University, which will be used as the testbed for the proposed control strategy. The built-in linear encoder has a position measurement resolution of 0.5 μm and a speed limit of 2 m/s, which enables us to perform high-speed/acceleration motion tests with acceleration more than 45 m/s^2 and velocity of 2 m/s. To further improve the position measurement resolution, a high-precision laser interferometer feedback system with a resolution of 20 nm is integrated into the testbed as well. Comparative experimental results for both the high-speed/acceleration motions and the slow motions using the external laser interferometer are presented to illustrate the excellent tracking performance of the proposed method.

II. Dynamic Models and Problem Formulation

The linear motors used in the commercial industrial gantry system considered here are current-controlled three-phase iron core motors driving linear positioning stages. In the derivation of the model, the electrical dynamics is neglected due to the much faster electric response—with the current amplifiers coming with the linear motors, the electrical dynamics has an offline estimated bandwidth in the kilohertz range. The mathematical model of each motor without considering any mechanical resonant modes can thus be described by

$$M\ddot{x} = u - F, \quad F = F_f + F_r + F_d \tag{1}$$

where x represents the position of the inertia load of the motor, M is the normalized[1] mass of the inertia load plus the coil assembly, u is the input voltage to the motor, F is the normalized lumped effect of uncertain nonlinearities such as friction force F_f, ripple force F_r and external disturbance F_d (e.g., cutting force in machining). While there have been many friction models proposed [4], a simple and often adequate approach is to regard friction force as a static nonlinear function of the velocity, i.e., $F_f(\dot{x})$, which is given by

$$F_f(\dot{x}) = B\dot{x} + F_{fn}(\dot{x}) \tag{2}$$

where B is an equivalent viscous friction coefficient of the system, F_{fn} is the nonlinear Columb friction term which can be modelled to include the Stribeck effect. In practice, the friction force may also depend on position x at low speeds. This phenomenon is still captured by (1), since the bounded variation of position-dependent friction can be lumped into the external disturbance F_d. In the above model, the magnetic saturation effect is ignored for simplicity, as the working range of the positioning stage is normally restricted to the linear region of the torque versus the dc command input voltage to the motor amplifier. Should the magnetic saturation effect become an issue, the nonlinear models of magnetic saturation presented in [2] and [17] may be used to come out a better description of the input behavior and similar analysis as presented in the paper can be carried out.

Let $y_r(t)$ be the reference motion trajectory, which is assumed to be known, bounded with bounded derivatives up to the third order. The objective is to synthesize a control input u such that the output $y = x$ tracks $y_r(t)$ as closely as possible in spite of various model uncertainties.

III. Adaptive Robust Control of Linear Motor Systems

A. Design Models and Assumptions

In this paper, it is assumed that the permanent magnets of the same linear motor are all identical and are equally spaced at a pitch of P. Thus, F_r is a periodic function of position x with a period of P, i.e., $F_r(x + P) = F_r(x)$, and it can be approximated quite accurately by the first several harmonic functions of the position, which is denoted as $\bar{F}_r(x)$ and represented by

$$\bar{F}_r(x) = A_r^T S_r(x) \tag{3}$$

where $A_r = [A_{r1s}, A_{r1c}, \ldots, A_{rqs}, A_{rqc}]^T \in R^{2q}$ is the vector of unknown weights, $S_r(x) = [\sin((2\pi/P)x), \cos((2\pi/P)x), \ldots, \sin((2\pi q/P)x), \cos((2\pi q/P)x)]^T$ is the known basis shape function, and q is the numbers of harmonics used

[1]Normalized with respect to the unit of voltage of the control input.

to approximate $F_r(x)$. The larger q is, the better $\bar{F}_r(x)$ approximates $F_r(x)$, but the larger number of parameters to be adapted. So a tradeoff has to be made based on the particular structure of a motor. For example, in [3], it was experimentally observed that the first, the third, and the fifth harmonics are the main harmonics in the force ripple waveform.

The same as in [22] and [25], a simple *continuous* friction model is used to approximate the usual static *discontinuous* friction model for model compensation; the model used in the paper is given by $\bar{F}_{fn} = A_f S_f(\dot{x})$, where the amplitude A_f is unknown, and $S_f(\dot{x})$ is a continuous function.

With the above ripple force and friction modelling, the linear motor dynamics (1) can be written as

$$M\ddot{x} = u - B\dot{x} - A_f S_f(\dot{x}) - A_r^T S_r(x) + d \tag{4}$$

where $d = (\bar{F}_{fn} - F_{fn}) + (\bar{F}_r - F_r) - F_d$.

In general, the system is subjected to parametric uncertainties due to the variations of M, B, A_f, A_r, and d_n, the nominal value of the lumped disturbance d. In order to use parameter adaptation to reduce parametric uncertainties for an improved performance, it is necessary to linearly parameterize the state space equation in terms of a set of unknown parameters. To achieve this, define the unknown parameter set $\theta = [\theta_1, \theta_2, \theta_3, \theta_{4b}^T, \theta_5]^T \in \mathbb{R}^{4+2q}$ as $\theta_1 = M$, $\theta_2 = B$, $\theta_3 = A_f$, $\theta_{4b} = A_r \in \mathbb{R}^{2q}$, and $\theta_5 = d_n$. Letting the two state variables x_1 and x_2 be the position and velocity, respectively, the state-space representation of (4) can thus be linearly parameterized in terms of θ as

$$\dot{x}_1 = x_2 \tag{5}$$

$$\theta_1 \dot{x}_2 = u - \theta_2 x_2 - \theta_3 S_f - \theta_{4b}^T S_r(x_1) + \theta_5 + \tilde{d} \tag{6}$$

where $\tilde{d} = d - d_n$.

For simplicity, in the following, the following notations are used: $\bullet_i$ for the ith component of the vector $\bullet$, $\bullet_{\min}$ for the minimum value of $\bullet$, and $\bullet_{\max}$ for the maximum value of $\bullet$. the operation $<$ for two vectors is performed in terms of the corresponding elements of the vectors. The following practical assumption is made.

Assumption 1: The extent of the parametric uncertainties and uncertain nonlinearities are known, i.e.,

$$\theta \in \Omega_\theta \triangleq \{\theta : \theta_{\min} < \theta < \theta_{\max}\} \tag{7}$$

$$\tilde{d} \in \Omega_d \triangleq \left\{\tilde{d} : |\tilde{d}| \le \delta_d\right\} \tag{8}$$

where $\theta_{\min} = [\theta_{1\min}, \cdots, \theta_{5\min}]^T$, $\theta_{\max} = [\theta_{1\max}, \cdots, \theta_{5\max}]^T$, and δ_d are known. ◇

B. Notations and Discontinuous Projection

Let $\hat{\theta}$ denote the estimate of θ and $\tilde{\theta}$ the estimation error (i.e., $\tilde{\theta} = \hat{\theta} - \theta$). In view of (7), the following adaptation law with discontinuous projection modification can be used:

$$\dot{\hat{\theta}} = \mathrm{Proj}_{\hat{\theta}}(\Gamma\tau) \tag{9}$$

where $\Gamma > 0$ is a diagonal matrix, τ is an adaptation function to be synthesized later. The projection mapping $\mathrm{Proj}_{\hat{\theta}}(\bullet) = [\mathrm{Proj}_{\hat{\theta}_1}(\bullet_1), \cdots, \mathrm{Proj}_{\hat{\theta}_5}(\bullet_5)]^T$ is defined as

$$\mathrm{Proj}_{\hat{\theta}_i}(\bullet_i) = \begin{cases} 0, & \text{if } \hat{\theta}_i = \theta_{i\max} \text{ and } \bullet_i > 0 \\ 0, & \text{if } \hat{\theta}_i = \theta_{i\min} \text{ and } \bullet_i < 0 \\ \bullet_i, & \text{otherwise.} \end{cases} \tag{10}$$

It can be shown [27] that for any adaptation function τ, the projection mapping used in (10) guarantees

$$\mathbf{P1} \quad \hat{\theta} \in \Omega_\theta \triangleq \{\hat{\theta} : \theta_{\min} \le \hat{\theta} \le \theta_{\max}\}$$

$$\mathbf{P2} \quad \tilde{\theta}^T\left(\Gamma^{-1}\mathrm{Proj}_{\hat{\theta}}(\Gamma\tau) - \tau\right) \le 0, \qquad \forall\tau. \tag{11}$$

C. ARC Controller Design

Noting that (5) does not have any uncertainties, an ARC Lyapunov function can thus be constructed for (5) and (6) directly. Define a switching-function-like quantity as

$$p = \dot{e} + k_1 e = x_2 - x_{2eq}, \qquad x_{2eq} \triangleq \dot{y}_d - k_1 e \tag{12}$$

where $e = y - y_d(t)$ is the output tracking error, $y_d(t)$ is the desired trajectory to be tracked by y, and k_1 is any positive feedback gain. If p is small or converges to zero exponentially, then the output tracking error e will be small or converge to zero exponentially since $G_p(s) = e(s)/p(s) = 1/(s + k_1)$ is a stable transfer function. So the rest of the design is to make p as small as possible. Differentiating (12) and noting (6), one obtains

$$\begin{aligned} M\dot{p} &= u - \theta_1 \dot{x}_{2eq} - \theta_2 x_2 - \theta_3 S_f - \theta_{4b}^T S_r + \theta_5 + \tilde{d} \\ &= u + \varphi^T\theta + \tilde{d} \end{aligned} \tag{13}$$

where $\dot{x}_{2eq} \triangleq \ddot{y}_d - k_1\dot{e}$ and $\varphi^T = [-\dot{x}_{2eq}, -x_2, -S_f(x_2), -S_r(x_1), 1]$. Noting the structure of (13), the following ARC control law is proposed:

$$u = u_a + u_s, \qquad u_a = -\varphi^T\hat{\theta} \tag{14}$$

where u_a is the adjustable model compensation needed for achieving perfect tracking, and u_s is a robust control law to be synthesized later. Substituting (14) into (13), and then simplifying the resulting expression, one obtains

$$M\dot{p} = u_s - \varphi^T\tilde{\theta} + \tilde{d}. \tag{15}$$

The robust control function u_s consists of two terms given by

$$u_s = u_{s1} + u_{s2}, \quad u_{s1} = -k_2 p \tag{16}$$

where u_{s1} is used to stabilize the nominal system, which is a simple proportional feedback with k_2 being the feedback gain in this case; u_{s2} is a robust feedback used to attenuate the effect of model uncertainties. Noting Assumption 1 and P1 of (11), there exists a u_{s2} such that the following two conditions are satisfied:

$$\begin{aligned} &\text{i} \quad p\{u_{s2} - \varphi^T\tilde{\theta} + \tilde{d}\} \le \varepsilon \\ &\text{ii} \quad pu_{s2} \le 0 \end{aligned} \tag{17}$$

where ε is a design parameter which can be arbitrarily small. Essentially, i of (17) shows that u_{s2} is synthesized to dominate the

model uncertainties coming from both parametric uncertainties $\tilde{\theta}$ and uncertain nonlinearities $\tilde{d}$, and ii of (17) is to make sure that u_{s2} is dissipating in nature so that it does not interfere with the functionality of the adaptive control part u_a.

Theorem 1: If the adaptation function in (9) is chosen as

$$\tau = \varphi p \tag{18}$$

then the ARC control law (14) guarantees the following.

1) In general, all signals are bounded. Furthermore, the positive definite function V_s defined by

$$V_s = \frac{1}{2}Mp^2 \tag{19}$$

is bounded above by

$$V_s \leq \exp(-\lambda t)V_s(0) + \frac{\varepsilon}{\lambda}\left[1 - \exp(-\lambda t)\right] \tag{20}$$

where $\lambda = 2k_2/\theta_{1\max}$.

2) If after a finite time t_0, there exist parametric uncertainties only (i.e., $\tilde{d} = 0, \forall t \geq t_0$), then, in addition to results in A, zero final tracking error is also achieved, i.e., $e \longrightarrow 0$ and $p \longrightarrow 0$ as $t \longrightarrow \infty$.

Proof: See Appendix 1.

Remark 1: One smooth example of u_{s2} satisfying (17) can be found in the following way. Let h be any smooth function satisfying

$$h \geq \|\theta_M\|\|\varphi\| + \delta_d \tag{21}$$

where $\theta_M = \theta_{\max} - \theta_{\min}$. Then, u_{s2} can be chosen as

$$u_{s2} = -\frac{1}{4\varepsilon}h^2 p. \tag{22}$$

Other smooth or continuous examples of u_{s2} can be worked out in the same way as in [24], [27], and [28]. ♢

D. Trajectory Initialization and Generation

It is seen from (20) that transient tracking error is affected by the initial value $V_s(0)$, which may depend on the controller parameters. To further reduce transient tracking error, the idea of trajectory initialization [14], [27], can be utilized. Namely, instead of simply letting the desired trajectory for the controller be the actual reference trajectory or position (i.e., $y_d(t) = y_r(t)$), $y_d(t)$ can be generated using a filter. For example, $y_d(t)$ can be generated by the following third-order stable system

$$y_d^{(3)} + \beta_1 y_d^{(2)} + \beta_2 y_d^{(1)} + \beta_3 y_d = y_r^{(3)} + \beta_1 y_r^{(2)} + \beta_2 y_r^{(1)} + \beta_3 y_r \tag{23}$$

with the initial conditions given by $y_d(0) = x_1(0)$, $\dot{y}_d(0) = \dot{x}_1(0)$, and $\ddot{y}_d(0) = \ddot{x}_1(0)$. By doing so, $V_s(0) = 0$ and the transient tracking error is reduced.

IV. Desired Compensation ARC (DCARC)

In the ARC design presented in Section III, the regressor φ in the model compensation u_a (14) and adaptation function τ (18) depend on states x_1 and x_2. Such an adaptation structure may have several potential implementation problems [25]. First, φ has to be calculated online based on the actual measurement of the velocity x_2. Thus, the effect of measurement noise may be severe, and a slow adaptation rate may have to be used, which in turn reduces the effect of parameter adaptation. Second, despite that the intention of introducing u_a is for model compensation, because of φ, u_a depends on the actual feedback of the states also. Although theoretically the effect of this added implicit feedback loop has been considered in the robust control law design as seen from condition i of (17), practically, there still exists certain interactions between the model compensation u_a and the robust control u_s as both strongly depend on the actual feedback of the states. This may complicate the controller gain tuning process in implementation. In [20], Sadegh and Horowitz proposed a desired compensation adaptation law, in which the regressor is calculated by desired trajectory information only. By doing so, the effect of measurement noise is reduced, and the regressor can be calculated offline to save online computation time if needed. The idea was then incorporated in the ARC design in [25]. In the following, the desired compensation ARC is applied on the linear motor system, and particular structure of the linear motor dynamics is utilized to obtain less restrictive conditions on the selection of robust feedback gains.

The proposed desired compensation ARC law and the adaptation function have the same form as (14) and (18), respectively, but with regressor φ substituted by the desired regressor φ_d

$$u = u_a + u_s, \quad u_a = -\varphi_d^T\hat{\theta}, \quad \tau = \varphi_d p \tag{24}$$

where $\varphi_d^T = [-\ddot{y}_d, -\dot{y}_d, -S_f(\dot{y}_d), -S_r(y_d), 1]$. Substituting (24) into (13), and noting $x_2 = \dot{y}_d + \dot{e}$, one obtains

$$\begin{aligned} M\dot{p} = {} & u_s - \varphi_d^T\tilde{\theta} + \tilde{d} \\ & + \underbrace{(\theta_1 k_1 - \theta_2)\dot{e} + \theta_3\left[S_f(\dot{y}_d) - S_f(x_2)\right] + \theta_{4b}^T\left[S_r(y_d) - S_r(x_1)\right]}. \end{aligned} \tag{25}$$

Comparing (26) with (15), it can be seen that three additional terms (underbraced) appear, which may demand a strengthened robust control function u_s for a robust performance. Applying Mean Value Theorem, we have

$$\begin{aligned} S_f(x_2) - S_f(\dot{y}_d) &= g_f(x_2, t)\dot{e} \\ S_r(x_1) - S_r(y_d) &= g_r(x_1, t)e \end{aligned} \tag{26}$$

where $g_f(x_2, t)$ and $g_r(x_1, t)$ are certain nonlinear functions. The strengthened robust control function u_s has the same form as (16)

$$u_s = u_{s1} + u_{s2}, \quad u_{s1} = -k_{s1}p \tag{27}$$

but with k_{s1} being a nonlinear gain large enough such that the matrix A defined below is positive definite

$$A = \begin{bmatrix} \alpha_1 & \alpha_2 \\ \alpha_2 & \alpha_3 \end{bmatrix}, \quad \begin{aligned} \alpha_1 &= k_{s1} - k_2 - \theta_1 k_1 + \theta_2 + \theta_3 g_f \\ \alpha_2 &= -\tfrac{1}{2}\left(k_1\theta_2 + k_1\theta_3 g_f - \theta_{4b}^T g_r\right) \\ \alpha_3 &= \tfrac{1}{2}Mk_1^3 \end{aligned} \tag{28}$$

and u_{s2} is required to satisfy the following constraints similar to (17):

$$\begin{aligned} &\text{i} \quad p\left\{u_{s2} - \varphi_d^T\tilde{\theta} + \tilde{d}\right\} \leq \varepsilon \\ &\text{ii} \quad pu_{s2} \leq 0. \end{aligned} \tag{29}$$

Specific form of u_{s2} can be obtained using the techniques in Remark 1. For example, similar to (22), it is chosen as

$$u_{s2} = -\frac{1}{4\varepsilon}h'^2 p \tag{30}$$

where h' is any function satisfying

$$h' \geq \|\theta_M\|\|\varphi_d\| + \delta_d. \tag{31}$$

Remark 2: It is easy to show that $A \geq 0$, if and only if the following condition is satisfied:

$$k_{s1} \geq k_2 + \theta_1 k_1 - \theta_2 - \theta_3 g_f + \frac{1}{2\theta_1 k_1^3} \times \left(\theta_2 k_1 + \theta_3 k_1 g_f + \left|\theta_{4b}^T g_r\right|\right)^2. \tag{32}$$

Theorem 2: If the DCARC law (24) is applied, then we get the following.

1) In general, all signals are bounded. Furthermore, the positive definite function V_s defined by

$$V_s = \frac{1}{2}Mp^2 + \frac{1}{2}Mk_1^2e^2 \tag{33}$$

is bounded above by

$$V_s \leq \exp(-\lambda t)V_s(0) + \frac{\varepsilon}{\lambda}\left[1 - \exp(-\lambda t)\right] \tag{34}$$

where $\lambda = \min\{2k_2/\theta_{1\max}, k_1\}$.

2) If after a finite time t_0, there exist parametric uncertainties only (i.e., $\tilde{d} = 0$, $\forall t \geq t_0$), then, in addition to results in 1), zero final tracking error is also achieved, i.e., $e \longrightarrow 0$ and $p \longrightarrow 0$ as $t \longrightarrow \infty$.

Proof: See Appendix 2.

Remark 3: In addition to the reduced effect of measurement noise and the reduced online computation time, the DCARC law (24) also has the following advantages.

1) Due to the use of projection mapping in (9), $\hat{\theta}$ is bounded as shown by P1 of (11). Thus the model compensation u_a in (24) is bounded no matter what type of adaptation law is going to be used. This implies the robust control function u_s may be synthesized totally independent from the design of parameter adaptation law for stability.
2) Gain tuning process becomes simpler since some of the bounds like the first term in the right-hand side of (31) can be estimated offline.

♢

Remark 4: It is noted that the condition on the selection of robust feedback gain k_{s1} is much less restrictive than those in [25]. This is achieved by judiciously selecting a p.d. function given by (33) instead of the general formulations in [25]. ♢

Remark 5: For motor system equipped with high-resolution position encoder, position measurement feedback is normally quite clean. Comparatively, the velocity measurement is very noisy, which significantly limits the achievable performance. To further alleviate the effect of this noisy velocity feedback, in implementation, the parameter estimates can be updated as follows. Let j represent the sampling instance, ΔT be the sampling period, γ_i be the ith diagonal element of Γ, $\varphi_{d,i}$ be the ith component of φ_d and $\Theta_i = \hat{\theta}_i(j\Delta T) + \gamma_i \int_{j\Delta T}^{(j+1)\Delta T} \varphi_{d,i} p\, dt$, then the digital implementation of the continuous adaptation law (9) with τ given by (24) is

$$\hat{\theta}_i\left[(j+1)\Delta T\right] = \begin{cases} \theta_{i\max}, & \text{if } \Theta_i > \theta_{i\max} \\ \theta_{i\min}, & \text{if } \Theta_i < \theta_{i\min} \\ \Theta_i, & \text{otherwise.} \end{cases} \tag{35}$$

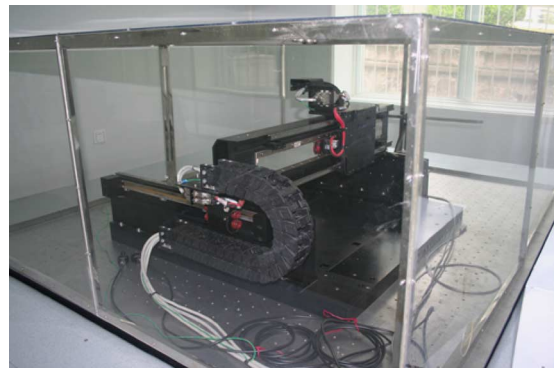

Fig. 1. Experimental setup.

The above digital implementation of parameter estimates needs the feedback of $p = \dot{e} + k_1 e$, which in turn needs the feedback of velocity x_2. Thus, the parameter estimates may be quite noisy if the measurement of the velocity x_2 is noisy. To bypass this problem, one can rewrite Θ_i as

$$\Theta_i = \hat{\theta}_i(j\Delta T) + \gamma_i \int_{j\Delta T}^{(j+1)\Delta T} \varphi_{d,i}(\dot{e} + k_1 e)dt. \tag{36}$$

Since $\varphi_d(t)$ depends on the reference trajectory only and its derivative $\dot{\varphi}_d(t)$ can be precomputed, one can integrate (36) by parts to obtain

$$\Theta_i = \hat{\theta}_i(j\Delta T) + \gamma_i \left(k_1 \int_{j\Delta T}^{(j+1)\Delta T} \varphi_{d,i} e\, dt + \varphi_{d,i} e \Big|_{j\Delta T}^{(j+1)\Delta T} - \int_{j\Delta T}^{(j+1)\Delta T} \dot{\varphi}_{d,i}(t) e\, dt \right). \tag{37}$$

Thus the parameter estimates implemented through (37) and (35) depend on the desired trajectory and output tracking error only, which are free of velocity measurement noise—another implementation advantage of DCARC. ♢

V. Comparative Experiments

A. Experiment Setup

To test the proposed nonlinear ARC strategy and study fundamental problems associated with high-speed/high-acceleration/high-accuracy motion control of iron-core linear motor drive systems, a two-axis X-Y Anorad HERC-510-510-AA1-B-CC2 gantry by Rockwell Automation is set up as a test-bed. As shown in Fig. 1, the two axes of the X-Y stage are mounted orthogonally with X-axis on top of Y-axis. The resolution of the encoders is 0.5 μm after quadrature. The velocity signal is obtained by the difference of two consecutive position measurements. Due to space limitation, in the following, only experimental results for X-axis are presented.

Standard least-square identification is performed to obtain the parameters of the X-axis. The approximate nominal values of

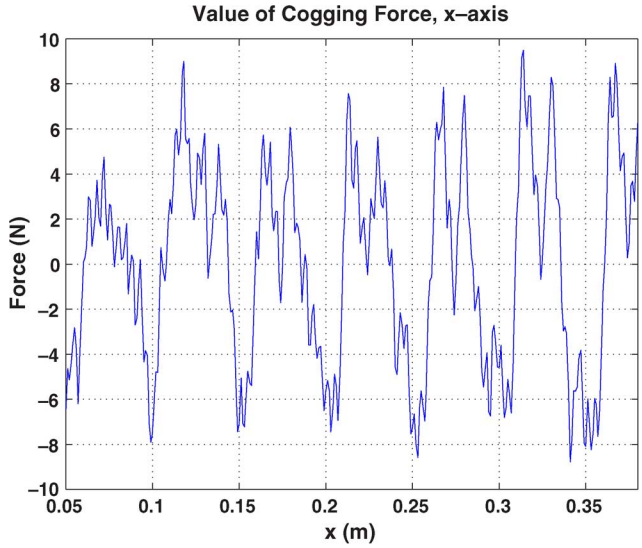

Fig. 2. Measurement of cogging forces.

M, B, and A_f are:[2] $\hat{\theta}_1 = 0.1$ (V/m/s^2), $\hat{\theta}_2 = 0.2$ (V/m/s), and $\hat{\theta}_3 = 0.1$ (V). Explicit measurement of cogging force is conducted for both axes by blocking the motor and using an external force sensor (HBM U10M Force Transducer with AE101 Amplifier) to measure the blocking forces at zero input voltages. This measurement is done for various positions with 1 mm incremental distance. The measured cogging force is shown in Fig. 2 versus the load position from $x = 0.05$ m to $x = 0.38$ m. Frequency domain analysis of the measured ripple forces indicates that the fundamental period corresponds to the pitch of the magnets ($P = 50$ mm) and that the second and third harmonics are the main harmonics. Thus the basis functions are chosen as

$$S_r(x_1) = \left[\sin\left(\frac{2\pi}{P}x_1\right), \cos\left(\frac{2\pi}{P}x_1\right), \sin\left(\frac{4\pi}{P}x_1\right), \cos\left(\frac{4\pi}{P}x_1\right), \sin\left(\frac{6\pi}{P}x_1\right), \cos\left(\frac{6\pi}{P}x_1\right)\right]^T. \quad (38)$$

It is noted that the unknown parameter θ_5 in (13) represents the nominal value of the lumped disturbance. In viewing result B of Theorem 1, theoretically, the bounds of θ_5 should be chosen as large as possible so that large disturbance can be compensated via the adjustable model compensation term u_a in (14). However, in practice, this should not be overdone, especially in the presence of control saturation. In fact, by choosing proper bounds of θ_5 based on the control saturation level, the proposed ARC may have a well designed built-in anti-integration windup mechanism due to the use of projection mapping in the parameter adaptation law (9). With this in mind, the bounds of the parameter variations are chosen as

$$\theta_{\min} = [0.08, \quad 0.15, \quad 0.08, \quad -0.1, \quad -0.1, \quad -0.1, \quad -0.1, \quad -0.1, \quad -0.1, \quad -0.5]^T$$
$$\theta_{\max} = [0.20, \quad 0.35, \quad 0.15, \quad +0.1, \quad +0.1, \quad +0.1, \quad +0.1, \quad +0.1, \quad +0.1, \quad +0.5]^T.$$

[2]All units are normalized in terms of the control input unit of voltage. The gain from the input voltage to the force applied to the mechanical system is computed as $k_f = 69$ N/V through the measurement of input voltage to the system and the resultant force when the motor is blocked.

B. Performance Index

The following performance indexes will be used to measure the quality of each control algorithm:

- $L_2[e] = \sqrt{(1/T_f)\int_0^{T_f} |e|^2 dt}$, the scalar valued L_2 norm of the tracking error history;
- $e_M = \max_t\{|e(t)|\}$, the maximal absolute value of the tracking error history.

C. Comparative Experimental Results

The control algorithms are implemented using a dSPACE DS1103 controller board. The controller executes programs at a sampling frequency $f_s = 5$ kHz, which results in a velocity measurement resolution of 0.0025 m/s.

In [22], experimental results have shown that DCARC achieves better performance than ARC in terms of all performance indexes. Thus in this paper, only DCARC algorithm is implemented and the focus is on the comparison of the following three controllers.

PID: PID controller with feedforward compensation given by

$$u = \hat{\theta}_1(0)\ddot{y}_d(t) + \hat{\theta}_2(0)\dot{y}(t) + \hat{\theta}_3(0)S_f(\dot{y}) - K_p e - K_i \int e\, dt - K_d \dot{e} \quad (39)$$

where $\hat{\theta}_1(0)$, $\hat{\theta}_2(0)$, and $\hat{\theta}_3(0)$ are the fixed parameter estimates chosen to be their offline estimated values of 0.1, 0.2, and 0.1 during no load experiments respectively. To see the link between the underlining controller structures of the conventional PID and the proposed DCARC, perform the following transformation by substituting $p = \dot{e} + k_1 e$ into (39):

$$\begin{aligned} u &= \hat{\theta}_1(0)\ddot{y}_d(t) + \hat{\theta}_2(0)\dot{y}(t) + \hat{\theta}_3(0)S_f(\dot{y}) - K_p e \\ &\quad - K_i \int \frac{p - \dot{e}}{k_1}\, dt - K_d p + K_d k_1 e \\ &= \hat{\theta}_1(0)\ddot{y}_d(t) + \hat{\theta}_2(0)\dot{y}(t) + \hat{\theta}_3(0)S_f(\dot{y}) \\ &\quad \times \left(-K_p + \frac{K_i}{k_1} + K_d k_1\right)e - K_d p - \frac{K_i}{k_1}\int p\, dt. \end{aligned} \quad (40)$$

By choosing

$$\begin{cases} -K_p + \frac{K_i}{k_1} + K_d k_1 = 0 \\ \frac{K_i}{k_1} = \gamma_5 \\ K_d = k_s \end{cases} \quad (41)$$

and letting

$$\dot{\hat{\theta}}_5 = \gamma_5 p \quad (42)$$

the PID control law (40) can be put into a form similar to the proposed DCARC (24)

$$u = u_a + u_s, \quad u_a = -\varphi^T\hat{\theta}, \quad u_s = -k_s p \quad (43)$$

where $\varphi^T = [-\ddot{y}_d, -\dot{y}, -S_f(\dot{y}), -S_r(y_d), 1]$ and $\hat{\theta} = [\hat{\theta}_1(0), \hat{\theta}_2(0), \hat{\theta}_3(0), 0, \hat{\theta}_5]^T$. It is thus clear that the proposed ARC can be thought as a generalization of the conventional PID controller with the following improvements: 1) using online parameter adaptation for physical parameters to deal with parametric uncertainties (i.e., $\hat{\theta}_1$, $\hat{\theta}_2$, and $\hat{\theta}_3$ are updated by (9) instead of being the constant offline estimates in (43); 2) having a built-in anti-integration windup mechanism (i.e., using the projection (10) for $\dot{\hat{\theta}}_5$ instead of the pure integration (42);

TABLE I
EXPERIMENTAL RESULTS

	set 1		
controller	PID	DCARC1	DCARC2
$e_M\,(\mu m)$	14.753	7.5479	14.920
$L_2[e]\,(\mu m)$	5.5050	2.1967	5.4707

TABLE II
EXPERIMENTAL RESULTS

	set 2		
controller	PID	DCARC1	DCARC2
$e_M\,(\mu m)$	19.285	6.4224	14.111
$L_2[e]\,(\mu m)$	7.7753	2.0617	5.5676

and 3) using the nonlinear robust feedback gains (27) and (30) instead of a constant feedback gain in (43) for a theoretically guaranteed global stability and robust performance.

The above equations establish the relationship between PID controller parameters and the proposed DCARC parameters, which are used in selecting the parameters of PID and DCARC to make the experimental results comparable. With the proposed ARC controller parameters being chosen as $k_1 = 300$, $k_s = 500 \times 0.1$, and $\gamma_5 = 1000$, from (41), $K_p = 16\,000$, $K_d = 50$, and $K_i = 300\,000$, which puts the resulting three closed-loop poles of the PID controller around $-240 \pm 304.7j$ and -19.9 for no-load situations.

DCARC1 (with force ripple compensation): The controller proposed in Section IV. The parameters of the controller are chosen as: $k_1 = 300$, $k_s = 500 \times 0.1$. The continuous function $S_f(x_2)$ is chosen as $(2/\pi)\arctan(1000x_2)$. The adaptation rates are set as $\Gamma = \mathbf{diag}\{1, 10, 10, 100, 100, 100, 100, 100, 100, 1000\}$. The initial parameter estimates are chosen as: $\hat{\theta}(0) = [0.1, 0.2, 0.1, 0, 0, 0, 0, 0, 0, 0]^T$.

DCARC2 (without force ripple compensation): The same control law as the above DCARC but without force ripple compensation, i.e., letting $\Gamma = \mathbf{diag}\{1, 10, 10, 0, 0, 0, 0, 0, 0, 1000\}$.

To test the tracking performance of the proposed algorithm, the following three typical reference trajectories are considered.

Case 1—Tracking a Sinusoidal Trajectory (Without Load and With Load): ***Comparative experiments are run for tracking a sinusoidal trajectory of*** $y_r = 0.15 \cdot sin(5t - (\pi/2)) + 0.15$. The desired trajectory y_d is generated by (23) in which $\beta_1 = 150$, $\beta_2 = 7500$, and $\beta_3 = 125\,000$. The following test sets are performed:

Set 1) to test the nominal tracking performance of the controllers, the motor is run without payload, which is equivalent to $\theta_1 = 0.1$;

Set 2) to test the performance robustness of the algorithms to parameter variations, a 5 kg payload is mounted on the motor.

The experimental results in terms of performance indexes are given in Tables I and II and the tracking errors are plotted in Figs. 3 and 4, respectively. As seen from these results, in terms of e_M and e_F, the performance of feedforward PID controller is similar to that of DCARC without force ripple compensation for set1, in which the system has the same value of load as the offline identification. But after a load of 5 kg is added, the performance of the feedforward PID controller deteriorates while the error of DCARC2 still remains the same level as the no-load situation due to its online parameter adaptation capability. This validates that the proposed DCARC algorithm has performance robustness under parametric uncertainties. Overall, no matter if the additional load is added or not, the tracking error of DCARC1 is always much smaller than the other two controllers, demonstrating the effectiveness of the proposed DCARC with cogging force compensation.

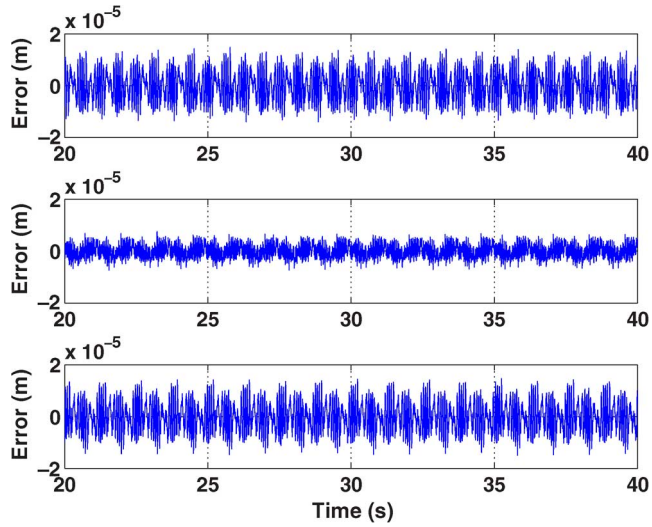

Fig. 3. Tracking errors (PID, DCARC1, and DCARC2, respectively), set1.

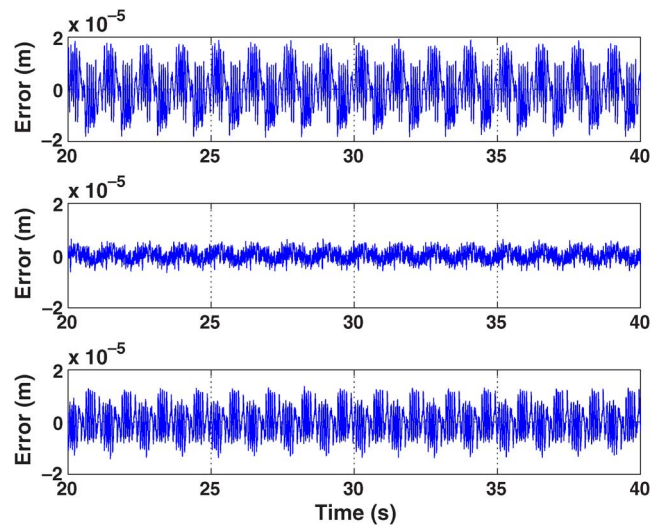

Fig. 4. Tracking errors (PID, DCARC1, and DCARC2, respectively), set2.

Case 2—High-Speed High-Acceleration Point-to-Point Motion Trajectory (Without Load and With Load): A fast point-to-point desired motion trajectory with high-acceleration/deceleration, which runs back and forth several times, is shown in Fig. 5. The trajectory has a maximum velocity of $v_{\max} = 2$ m/s and a maximum acceleration of $a_{\max} = 40$ m/s^2. The tracking errors of PID, DCARC1, and DCARC2 are shown in Fig. 6, and the magnified error plots over the constant speed period of one run are shown in Fig. 7. As seen, both DCARC controllers achieve much better performance than PID does. Furthermore, during the constant speed period of motion, the tracking error

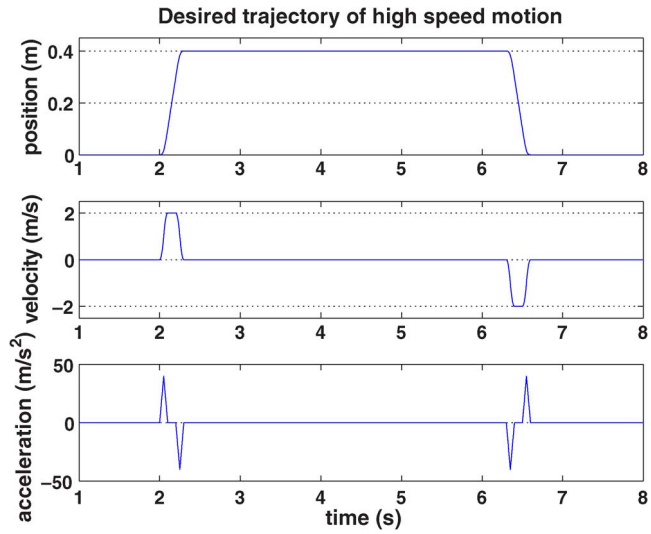

Fig. 5. Desired trajectory of a high-speed high-acceleration motion (2 m/s maximum speed and 40 m/s^2 maximum acceleration).

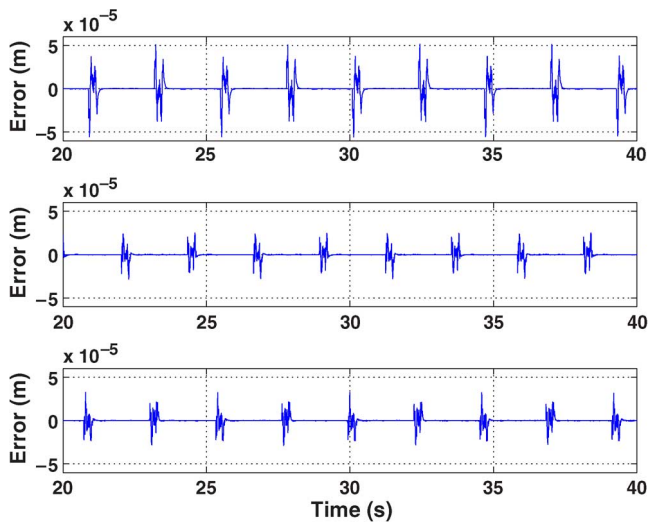

Fig. 6. Tracking errors of PID, DCARC1, and DCARC2 in high-speed/high-acceleration motion (2 m/s maximum speed and 40 m/s^2 maximum acceleration).

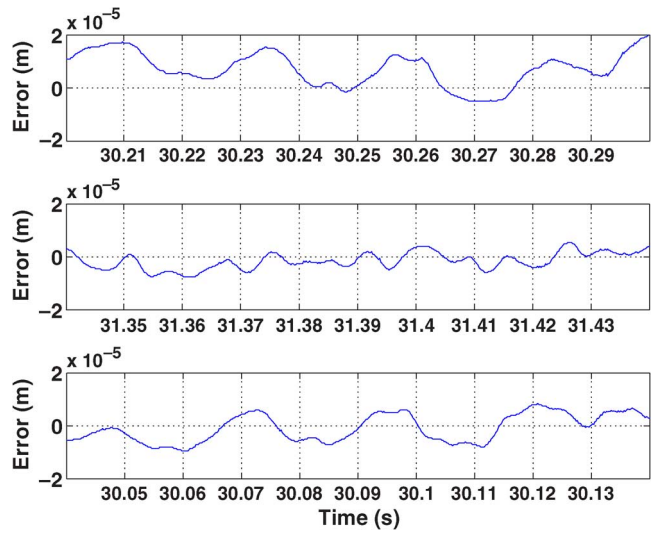

Fig. 7. Magnified error plots over constant speed period of one run (PID, DCARC1, and DCARC2, respectively) (2 m/s maximum speed and 40 m/s^2 maximum acceleration).

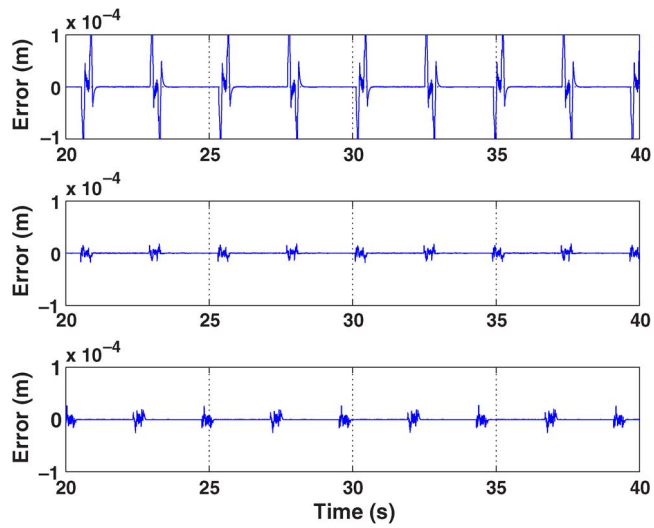

Fig. 8. Tracking errors of PID, DCARC1, and DCARC2 in high-speed motion with 5 kg payload (1.5 m/s maximum speed and 20 m/s^2 maximum acceleration).

of DCARC1 is smaller than that of DCARC2, validating the effectiveness of using cogging force compensation.

To test the performance robustness of the algorithms to parameter variations, a 5 kg payload is mounted on the motor. With a 5 kg payload, the maximum acceleration of the desired trajectory has to been made smaller as otherwise the desired input will be very close to the saturation level of the control input. Thus in experiments, the maximum acceleration and the maximum velocity of the desired trajectory are reduced to $a_{\max} = 20$ m/s^2 and $v_{\max} = 1.5$ m/s, respectively. The tracking errors of PID, DCARC1, and DCARC2 are shown in Fig. 8, and the magnified error plots over the constant speed period of one run are shown in Fig. 9. As can be seen from these plots, during the acceleration/deceleration periods, the performance of PID controller becomes extremely bad with the added payload. However, the performances of two DCARCs are as good as in the no-payload case. This well illustrates the importance of online parameter adaptation when true values of the parameters are significantly different from their nominal ones and the performance robustness of the proposed DCARC.

Case 3—Extreme Low-Speed Point-to-Point Motion Trajectory (Without Load and With Load): The proposed DCARC1 is also tested for extreme low speed short distance movements. The desired trajectories are of the same point-to-point type movement, but with extreme low constant speeds of 0.02, 0.002, and 0.0002 m/s, respectively. The maximum accelerations are set at 0.5, 0.05 , and 0.005 m/s^2, and the travel distances are 0.1, 0.01, and 0.001 m, respectively. For these experiments, the built-in linear encoder feedback of the gantry is not good enough any more. Instead, the external laser interferometer is used for the position measurement with a resolution of 20 nm. Again, the algorithms are tested for two experimental settings: systems without payload and systems with 5 kg payload.

Fig. 10 shows the tracking errors of the three experiments for the no-payload case with the blowout portions for the constant speed part shown in Fig. 11. Fig. 12 shows the tracking er-

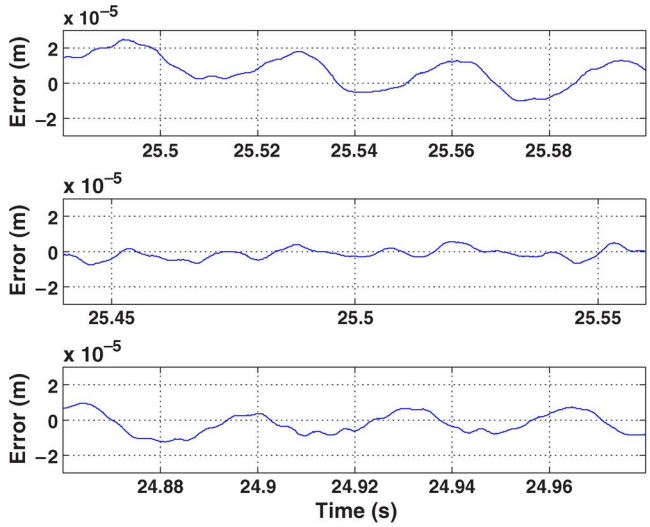

Fig. 9. Magnified error plots over constant speed period of one run (PID, DCARC1, and DCARC2 respectively) with 5 kg payload (1.5 m/s maximum speed and 20 m/s^2 maximum acceleration).

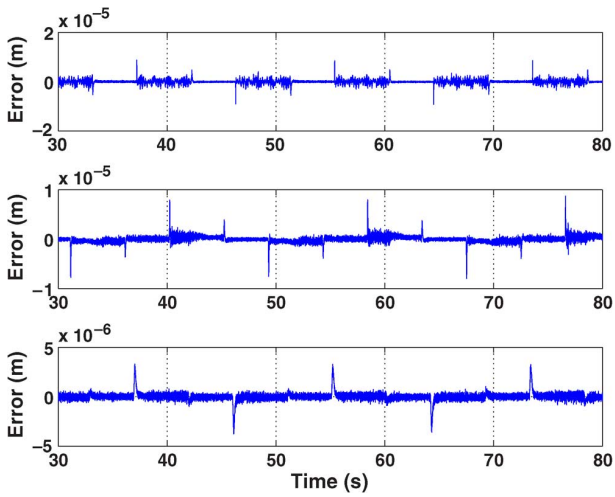

Fig. 10. Low speed experiments for no-payload case.

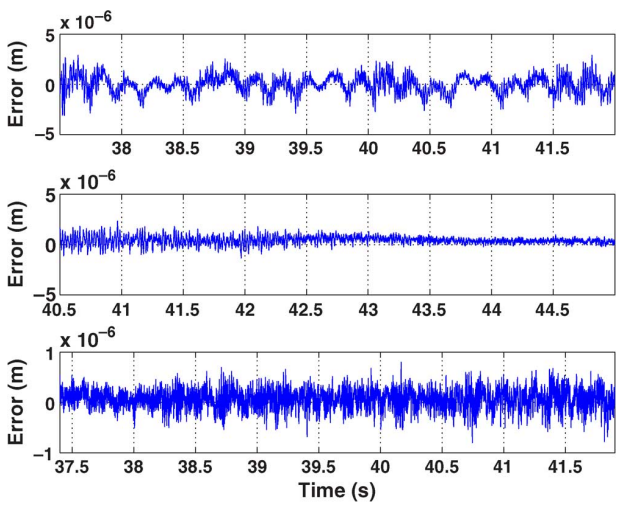

Fig. 11. Low speed experiments for no-payload case (constant speed portion).

rors of all three experiments with the 5-kg payload case with the blowout portions for the constant speed part shown in Fig. 13. The proposed DCARC1 algorithm achieves good performances

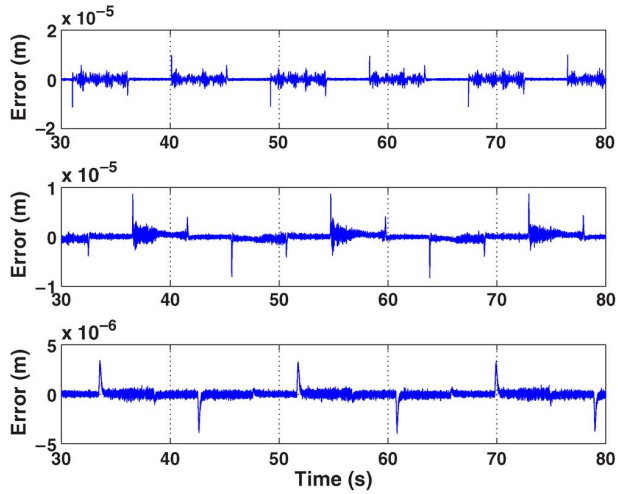

Fig. 12. Low speed experiments for 5-kg payload case.

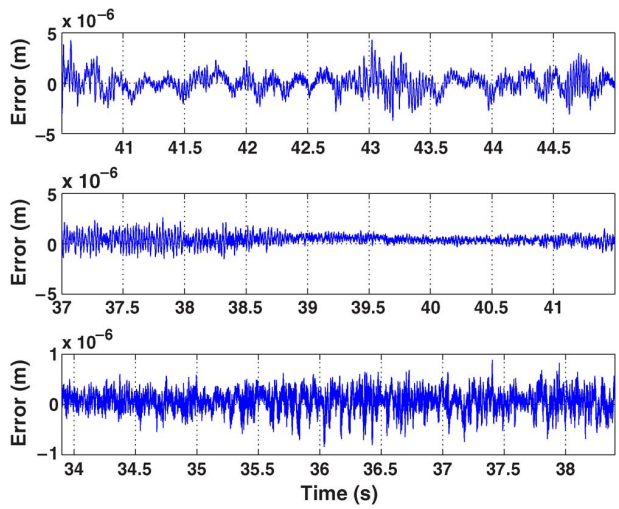

Fig. 13. Low speed experiments for 5-kg payload case (constant speed portion).

in both no-payload and 5-kg payload cases. The errors in acceleration and deceleration periods are within 10 μm and the errors in constant speed motion period are within 3 μm for all the three desired trajectories with various maximum speeds. For the extreme low speed of 0.0002 m/s case, the tracking errors during the constant speed portions are typically within a few hundred nanometers. These results demonstrate the good tracking performance of the proposed DCARC with cogging force compensation for low-speed motions as well.

VI. Conclusion

In this paper, a desired compensation ARC controller with ripple force compensation has been developed for high performance robust motion control of linear motors. The proposed controller takes into account the effect of model uncertainties coming from the inertia load, friction force, force ripple, and external disturbances. In particular, based on the special structure of the ripple forces, design models consisting of known basis functions with unknown weights are used to approximate the unknown nonlinear ripple forces. Online parameter adaptation is then utilized to reduce the effect of various parametric uncertainties while the uncompensated uncertain nonlinearities are handled effectively via certain robust control laws for high

performance. As a result, time-consuming and costly rigorous offline identification of friction and ripple forces is avoided without sacrificing tracking performance. Furthermore, it is shown that the desired compensation ARC scheme, in which the regressor is calculated using reference trajectory information only, offers several implementation advantages such as less online computation time, reduced effect of measurement noise, a separation of robust control design from parameter adaptation, and a faster adaptation rate in implementation. Comparative experimental results are obtained for tracking different types of reference trajectories on an iron core linear motor. Experimental results verify the high-performance nature of the proposed scheme.

APPENDIX I

Proof of Theorem 1: From (15) and (16), the derivative of V_s is given by

$$\dot{V}_s = -k_2 p^2 + p\{u_{s2} - \varphi^T \tilde{\theta} + \tilde{d}\}. \tag{44}$$

Noting condition i of (17), and choosing $\lambda = \min\{2k_2/\theta_{1\max}\}$, we have

$$\dot{V}_s \le -k_2 p^2 + \varepsilon \le -\lambda V_s + \varepsilon \tag{45}$$

which leads to (20) and thus proves the results in A of Theorem 1. Now consider the situation in B of Theorem 1, i.e., $\tilde{d} = 0, \forall t \ge t_0$. Choose a p.d. function V_a as

$$V_a = V_s + \frac{1}{2}\tilde{\theta}^T \Gamma^{-1} \tilde{\theta}. \tag{46}$$

From (44), condition ii of (17) and P2 of (11), the derivative of V_a satisfies

$$\dot{V}_a = \dot{V}_s + \tilde{\theta}^T \Gamma^{-1} \dot{\tilde{\theta}} \le -k_2 p^2 + \tilde{\theta}^T \Gamma^{-1}(\dot{\hat{\theta}} - \Gamma\tau) \le -k_2 p^2. \tag{47}$$

Therefore, $p \in L_2$. It is easy to check that $\dot{p}$ is bounded. So, p is uniformly continuous. By Barbalat's lemma, $p \longrightarrow 0$ as $t \longrightarrow \infty$. □

APPENDIX II

Proof of Theorem 2: Along the trajectory of (26), the time derivative of V_s given by (33) is

$$\dot{V}_s = p\Big\{u_s - \varphi_d^T \tilde{\theta} + (\theta_1 k_1 - \theta_2)\dot{e} + \theta_3 [S_f(\dot{y}_d) - S_f(x_2)] + \theta_{4b}^T [S_r(y_d) - S_r(x_1)] + \tilde{d}\Big\} + M k_1^2 e\dot{e} \tag{48}$$

Applying (26) and (27), and noting $\dot{e} = p - k_1 e$ and $\theta_1 = M$, we have

$$\dot{V}_s \le p\Big\{u_{s2} - \varphi_d^T \tilde{\theta} + \tilde{d}\Big\} + (-k_{s1} + \theta_1 k_1 - \theta_2 - \theta_3 g_f)p^2 + \left(\theta_2 k_1 + \theta_3 k_1 g_f - \theta_{4b}^T g_r\right) ep - M k_1^3 e^2. \tag{49}$$

If A given by (28) is p.d., then

$$\dot{V}_s \le p\Big\{u_{s2} - \varphi_d^T \tilde{\theta} + \tilde{d}\Big\} - k_2 p^2 - \frac{1}{2} M k_1^3 e^2. \tag{50}$$

With condition i of (29) and $\lambda = \min\{2k_2/\theta_{1\max}, k_1\}$, the derivative of V_s becomes

$$\dot{V}_s \le -\lambda V_s + \varepsilon \tag{51}$$

which leads to (34) and the results in A of Theorem 2 is proved. Now consider the situation in B of Theorem 2, i.e., $\tilde{d} = 0, \forall t \ge t_0$. Choose a p.d. function V_a as

$$V_a = V_s + \frac{1}{2}\tilde{\theta}^T \Gamma^{-1} \tilde{\theta}. \tag{52}$$

From (50), condition ii of (29), and P2 of (11), the derivative of V_a satisfies

$$\dot{V}_a = \dot{V}_s + \tilde{\theta}^T \Gamma^{-1} \dot{\tilde{\theta}} \le -k_2 p^2 - \frac{1}{2} M k_1^3 e^2 + \tilde{\theta}^T \Gamma^{-1}(\dot{\hat{\theta}} - \Gamma\tau) \le -W \tag{53}$$

where $W = k_2 p^2 + (1/2) M k_1^3 e^2$. Therefore, $W \in L_1$ and $V_a \in L_\infty$. Since all signals are bounded, it is easy to check that $\dot{W}$ is bounded and thus uniformly continuous. By Barbalat's lemma, $W \longrightarrow 0$ as $t \longrightarrow \infty$, which implies conclusion B of Theorem 2. □

ACKNOWLEDGMENT

The authors would like to thank Z. Chen for his help in obtaining the experimental results in this paper.

REFERENCES

[1] D. M. Alter and T. C. Tsao, "Control of linear motors for machine tool feed drives: Design and implementation of h_∞ optimal feedback control," *ASME J. Dyn. Syst., Meas., Control*, vol. 118, pp. 649–656, 1996.

[2] S. A. Bortoff, R. R. Kohan, and R. Milman, "Adaptive control of variable reluctance motors: A spline function approach," *IEEE Trans. Ind. Electron.*, vol. 45, no. 3, pp. 433–444, May/Jun. 1998.

[3] P. V. Braembussche, J. Swevers, H. V. Brussel, and P. Vanherck, "Accurate tracking control of linear synchronous motor machine tool axes," *Mechatron.*, vol. 6, no. 5, pp. 507–521, 1996.

[4] C. C. de Wit, H. Olsson, K. J. Astrom, and P. Lischinsky, "A new model for control of systems with friction," *IEEE Trans. Autom. Control*, vol. 40, no. 3, pp. 419–425, Mar. 1995.

[5] H. Fujimoto and B. Yao, " Multirate adaptive robust control for discrete-time non-minimum phase systems and application to linear motors," *IEEE/ASME Trans. Mechantron.*, vol. 10, no. 4, pp. 371–377, Aug. 2005.

[6] Y. Hong and B. Yao, " A globally stable high performance adaptive robust control algorithm with input saturation for precision motion control of linear motor drive system," *IEEE/ASME Trans. Mechatron.*, vol. 12, no. 2, pp. 198–207, Apr. 2007.

[7] Y. Hong and B. Yao, "A globally stable saturated desired compensation adaptive robust control for linear motor systems with comparative experiments," *Automatica*, vol. 43, no. 10, pp. 1840–1848, 2007.

[8] C. Hu, B. Yao, and Q. Wang, "Coordinated adaptive robust contouring controller design for an industrial biaxial precision gantry," *IEEE/ASME Trans. Mechatron.*, vol. 15, no. 5, pp. 728–735, Oct. 2010.

[9] C. Hu, B. Yao, and Q. Wang, "Integrated direct/indirect adaptive robust contouring control of a biaxial gantry with accurate parameter estimations," *Automatica*, vol. 46, no. 4, pp. 701–707, 2010.

[10] C.-I. Huang and L.-C. Fu, "Adaptive approach to motion controller of linear induction motor with friction compensation," *IEEE/ASME Trans. Mechatron.*, vol. 12, no. 4, pp. 480–490, Aug. 2007.

[11] J. Y. Hung and Z. Ding, "Design of currents to reduce torque ripple in brushless permanent magnet motors," *IEE Proc. B. Electric Power Appl..*, vol. 140, no. 4, pp. 260–266, Jul. 1993.

[12] P. A. Ioannou and J. Sun, *Robust Adaptive Control*. Englewood Cliffs, NJ: Prentice-Hall, 1996.
[13] S. Komada, M. Ishida, K. Ohnishi, and T. Hori, " Disturbance observer-based motion control of direct drive motors," *IEEE Trans. Energy Conv.*, vol. 6, no. 3, pp. 553–559, Sep. 1991.
[14] M. Krstic, I. Kanellakopoulos, and P. V. Kokotovic, *Nonlinear and Adaptive Control Design*. New York: Wiley, 1995.
[15] L. Lu, B. Yao, Q. Wang, and Z. Chen, "Adaptive robust control of linear motors with dynamic friction compensation using modified lugre model," *Automatica*, vol. 45, no. 12, pp. 2890–2896, 2009.
[16] R. Milman and S. Bortoff, "Observer-based adaptive control of a variable reluctance motor: Experimental results," *IEEE Trans. Control Syst. Technol.*, vol. 7, no. 5, pp. 613–621, Sep. 1999.
[17] R. T. Novotnak, J. Chiasson, and M. Bodson, "High-performance motion control of an induction motor with magnetic saturation," *IEEE Trans. Control Syst. Technol.*, vol. 7, no. 3, pp. 315–327, May 1999.
[18] G. Otten, T. Vries, J. Amerongen, A. Rankers, and E. Gaal, "Linear motor motion control using a learning feedforward controller," *IEEE/ASME Trans. Mechatron.*, vol. 2, no. 3, pp. 179–187, Sep. 1997.
[19] J. S. Reed and P. A. Ioannou, "Instability analysis and robust adaptive control of robotic manipulators," *IEEE Trans. Robot. Autom.*, vol. 5, no. 3, pp. 381–386, Jun. 1989.
[20] N. Sadegh and R. Horowitz, "Stability and robustness analysis of a class of adaptive controllers for robot manipulators," *Int. J. Robot. Res.*, vol. 9, no. 3, pp. 74–92, 1990.
[21] L. Xu and B. Yao, "Adaptive robust precision motion control of linear motors with ripple force compensation: Theory and experiments," in *Proc. IEEE Conf. Control Appl.*, 2000, pp. 373–378.
[22] L. Xu and B. Yao, "Adaptive robust precision motion control of linear motors with negligible electrical dynamics: Theory and experiments," *IEEE/ASME Trans. Mechatron.*, vol. 6, no. 4, pp. 444–452, 2001.
[23] L. Xu and B. Yao, "Output feedback adaptive robust precision motion control of linear motors," *Automatica*, vol. 37, no. 7, pp. 1029–1039, 2001.
[24] B. Yao, "High performance adaptive robust control of nonlinear systems: A general framework and new schemes," in *Proc. IEEE Conf. Decision Control*, 1997, pp. 2489–2494.
[25] B. Yao, "Desired compensation adaptive robust control," *ASME J. Dyn. Syst., Meas., Control*, vol. 131, no. 6, pp. 1–7, 2009.
[26] B. Yao, M. Al-Majed, and M. Tomizuka, " High performance robust motion control of machine tools: An adaptive robust control approach and comparative experiments," *IEEE/ASME Trans. Mechatron.*, vol. 2, no. 2, pp. 63–76, Jun. 1997.
[27] B. Yao and M. Tomizuka, "Smooth robust adaptive sliding mode control of robot manipulators with guaranteed transient performance," *ASME J. Dyn. Syst., Meas., Control*, vol. 118, no. 4, pp. 764–775, 1996.
[28] B. Yao and M. Tomizuka, "Adaptive robust control of SISO nonlinear systems in a semi-strict feedback form," *Automatica*, vol. 33, no. 5, pp. 893–900, 1997.
[29] B. Yao and M. Tomizuka, "Adaptive robust control of MIMO nonlinear systems in semi-strict feedback forms," *Automatica*, vol. 37, no. 9, pp. 1305–1321, 2001.
[30] S. Zhao and K. Tan, "Adaptive feedforward compensation of force ripples in linear motors," *Control Eng. Pract.*, vol. 13, pp. 1081–1092, 2005.

Bin Yao (S'92–M'96–SM'09) received the M.Eng. degree in electrical engineering from the Nanyang Technological University, Singapore, in 1992, the B.Eng. degree in applied mechanics from the Beijing University of Aeronautics and Astronautics, Beijing, China, in 1987, and the Ph.D. degree in mechanical engineering from the University of California at Berkeley, in 1996.

Since 1996, he has been with the School of Mechanical Engineering, Purdue University, West Lafayette, IN, where he was promoted to the rank of Associate Professor in 2002 and Professor in 2007. He was honored as a Kuang-piu Professor in 2005 and a Chang Jiang Chair Professor in 2010 at the Zhejiang University, Hangzhou, China, as well. His research interests include the design and control of intelligent high performance coordinated control of electro-mechanical/hydraulic systems, optimal adaptive and robust control, nonlinear observer design and neural networks for virtual sensing, modeling, fault detection, diagnostics, and adaptive fault-tolerant control, and data fusion. He has published significantly on the subjects with well over 150 technical papers while enjoying the application of the theory through industrial consulting.

Dr. Yao was a recipient of a Faculty Early Career Development (CAREER) Award from the National Science Foundation (NSF) in 1998, a Joint Research Fund for Outstanding Overseas Chinese Young Scholars from the National Natural Science Foundation of China (NSFC) in 2005, a Chang Jiang Chair Professorship from the Ministry of Education of China in 2010, the O. Hugo Schuck Best Paper (Theory) Award from the American Automatic Control Council in 2004, and the Outstanding Young Investigator Award of ASME Dynamic Systems and Control Division (DSCD) in 2007. He is a member of ASME and has chaired numerous sessions and served in a number of International Program Committee of various IEEE, ASME, and IFAC conferences including the General Chair of the 2010 IEEE/ASME International Conference on Advanced Intelligent Mechatronics. From 2000 to 2002, he was the Chair of the Adaptive and Optimal Control Panel and, from 2001 to 2003, the Chair of the Fluid Control Panel of the ASME Dynamic Systems and Control Division (DSCD). He is currently the Chair of the ASME DSCD Mechatronics Technical Committee he initiated in 2005. He was a Technical Editor of the IEEE/ASME TRANSACTIONS ON MECHATRONICS from 2001 to 2005, and has been an Associate Editor of the *ASME Journal of Dynamic Systems, Measurement, and Control* since 2006. More detailed information can be found at the Website: https://engineering.purdue.edu/~byao.

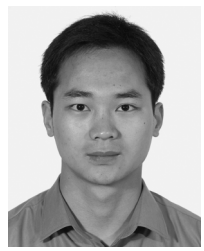

Chuxiong Hu received the B.Eng. degree from Zhejiang University, Hangzhou, China, in 2005, where he is currently pursuing the Ph.D. degree in mechatronic control engineering.

His research interests include coordinated motion control, precision mechatronics, adaptive control, robust control, and nonlinear systems.

Lu Lu received the B.Eng. degree in mechatronic control engineering from Zhejiang University, Zhejiang, China, in 2008. He is currently pursuing the Ph.D. degree from the School of Mechanical Engineering, Purdue University, West Lafayette, IN.

Qingfeng Wang received the M.Eng. and Ph.D. degrees in mechanical engineering from Zhejiang University, Hangzhou, China, in 1988 and 1994, respectively.

In 1994, he became a faculty member with Zhejiang University, where he was promoted to the rank of Professor in 1999. He was the Director of the State Key Laboratory of Fluid Power Transmission and Control at Zhejiang University from 2001 to 2005 and currently serves as the Director of the Institute of Mechatronic Control Engineering. His research interests include the electro-hydraulic control components and systems, hybrid power system and energy saving technique for construction machinery, and system synthesis for mechatronic equipments.